shown as points and calculated trajectory is shown as the corresponding line, demonstrating excellent agreement with the data. For the coordinate system defined Fig. 2(d), particles are considered removed if $x(z=-6\mu m)>6\mu m$.

Due to the variations of flow speed and the optical mode intensity across the channel, the lateral position of a particle as it approaches the T-intersection affects its final location. Particles approaching the intersection with x≈6μm are sorted almost instantly regardless of the size of the power, whereas particles of the same size with x≈-6μm need to move a lot farther along x and therefore may not get sorted. As seen in Fig. 2(e) this effect applies for all bead sizes, but is more significant for the 0.25μm beads due to the smaller effect of the optical force.

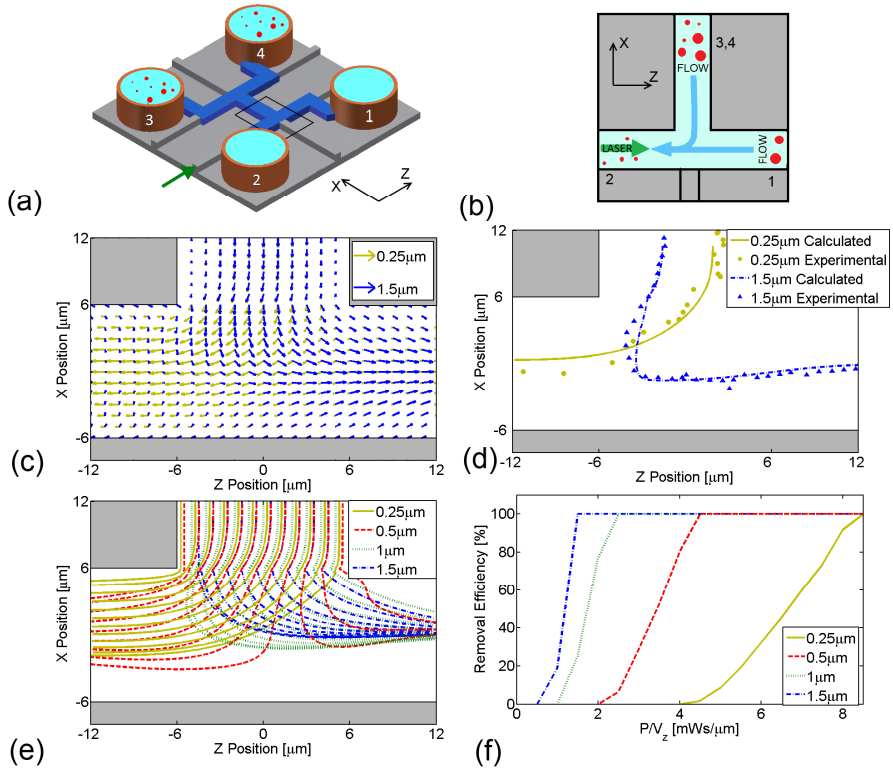

Fig. 3. The counterpropagating orientation (0.25μm is gold, 0.5μm is red, 1μm is green and 1.5μm is blue). See Media 3 and Media 4 for videos in this orientation. (a) Chip layout. (b) Orientation of Laser and Flows. (c) Flow and Laser are combined to create a velocity field. (d) Flow trajectories of beads in channel (points are experimental and lines are calculated). (e) Calculated trajectories of beads in an array of starting locations with $v_z = v_x = 10$ μm/s and P = 25mW for the counterpropagating orientation. For the 0.25μm, 0.5μm, 1μm, and 1.5μm beads, 0%, 25%, 100% and 100% are sorted respectively. (f) Calculated particle removal efficiencies with $v_z/v_x = 0.7$.

By comparing the number of beads that are removed from the flow to the total number of particles of that size, we calculate particle removal efficiency. By systematically varying the experimental conditions (flow speed, laser power), the comprehensive removal efficiency plot shown in Fig. 2(f) was created. Because the particle sorting effect is due to the difference in flow velocity compared to the velocity created by the laser, it is the relative ratio of flow velocity to power that characterizes a given parameter set. In addition, non-zero fluid flow into the horizontal channel (denoted by $v_x>0$) increases particle removal efficiency by directly

#201006 - $15.00 USD Received 8 Nov 2013; revised 6 Dec 2013; accepted 7 Dec 2013; published 23 Dec 2013

removing particles from the vertical channel. The strength of this effect increases with the ratio of v_x to the vertical input flow v_z.

Figure 2(f) shows particle removal efficiency with v_x/v_z = 0.3. Qualitatively good agreement between experiment and theory is found. The theory lines are not perfectly smooth due to the finite number of particles and lateral positions that were simulated. At low laser power, a finite and nearly size-independent removal probability is observed due to the presence of finite flow along the x-direction. As the laser power is increased, the removal efficiency can be tuned smoothly for each particle size, leading to full removal of progressively smaller particles. However, there will always be a finite fraction of smaller particles that is removed. Therefore, this geometry is best suited for tuning particle concentrations in mixtures where the complete removal of one species is not desired.

In the second ("counterpropagating") layout (see Fig. 3(a) and 3(b)), the chip is rotated to allow laser propagation along the liquid channel between reservoirs 1 and 2, with input flow adjusted to move beads from reservoir 3 (and/or reservoir 4) towards reservoir 2. In addition, a flow in the negative z-direction is introduced from reservoir 1 to reservoir 2. The laser force then acts to push larger beads along z towards reservoir 1, while smaller particles follow the flow and proceed to reservoir 2. See Media 3 for a video of this orientation in action (Media 4 shows the same video with contrast enhancement to make the beads easier to see). Particle trapping is also possible with this layout.

Depending on the relative values of both flow velocities and the power of the laser, beads at different locations will move in different directions (see Fig. 3(c)). Actual and calculated trajectories are compared in Fig. 3(d) where the 0.25μm (gold) beads continue in the direction of the flow whereas the 1.5μm (blue) beads are sorted. The criterion for sorting in this case is if a particle reaches $z = 6\mu m$. While the process is governed by the same physical principles as the orthogonal orientation, the effect of initial lateral position in the channel on particle removal is significantly weaker for the counterpropagating orientation since particles continue to feel the effects of the laser as they proceed along the negative z-direction (see Fig. 3(e)). In contrast to the orthogonal orientation, no particles are removed without optical power due to the different flow geometry (see Fig. 3(f)). Again, we find an increasing removal efficiency with optical power for each particle size. However, in this geometry it is possible to completely remove all particles above a selectable size out of a mixture while not removing any of the smaller sizes. Therefore, this geometry is best suited for selectively sorting a set of particle sizes from a stream. If combined with a second T-intersection, a "notch filter" could be created that selects only particles within a narrow size range.

3. Conclusion

We have introduced a method of combining pressure-based flow and optical forces in liquid-core waveguides to implement particle sorting on an optical chip. The particle removal process is automatic inasmuch as it does not require any feedback. We have demonstrated two implementations of this scheme on a single chip; one being ideal for adjusting relative particle concentrations, and one suited for eliminating all particles above a certain size from the stream. The relative concentrations and cutoff sizes can be tuned using laser power and/or flow speed. While we have focused on identical particles of different size in this work, this scheme could also be applied to select particles based on their refractive index or due to differences in shape. The simplicity of the schemes and the planar nature of the optofluidic chip suggest that this technique can be used for up-stream sample processing of liquid analytes for subsequent optical sensing and analysis on a single chip.

Acknowledgments

We would like to acknowledge the early efforts of J. McDowell on the simulations used in this research. This work was supported by NIH/NIBIB under grant 1R21EB008802, and the W. M. Keck Center for Nanoscale Optofluidics at UCSC.

#201006 - $15.00 USD Received 8 Nov 2013; revised 6 Dec 2013; accepted 7 Dec 2013; published 23 Dec 2013